R. & M. No. 2743
(13,207)
A.R.C. Technical Report

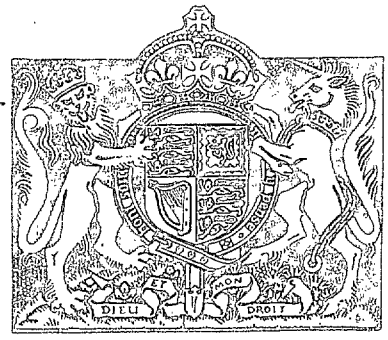

MINISTRY OF SUPPLY

AERONAUTICAL RESEARCH COUNCIL
REPORTS AND MEMORANDA

Tests Related to the Effect of Profile Shape and Camber-Line on Compressor Cascade Performance

By

S. J. ANDREWS, B.Sc.(Eng.)

LONDON: HER MAJESTY'S STATIONERY OFFICE
1955
PRICE 6*s* 6*d* NET

Tests Related to the Effect of Profile Shape and Camber-Line on Compressor Cascade Performance

By

S. J. ANDREWS, B.Sc.(Eng.)

COMMUNICATED BY THE PRINCIPAL DIRECTOR OF SCIENTIFIC RESEARCH (AIR), MINISTRY OF SUPPLY

Reports and Memoranda No. 2743*

October, 1949

Summary.—Cascade tests have been made to obtain information on the related questions of whether simpler sections than the normal aerofoil C4 can be used without loss of efficiency, and whether a particular section should be constructed on a circular-arc or a parabolic-arc camber-line. Of the large possible number of simple shapes, three only were chosen for comparison with the aerofoil. They were a flat plate with rounded leading and trailing edges, a flat plate with sharpened leading and trailing edges, and an approximately biconvex shape. A representative cascade shape was chosen (blade inlet angle 55 deg, outlet angle 30 deg, and pitch/chord ratio 0·75) and four cascades with the four sections mentioned above mounted on circular-arc camber-lines were made up. In addition, to provide data on the relative advantage of circular-arc and parabolic-arc camber-line, two cascades were made up on parabolic-arcs.

The main conclusions to be drawn are that the approximately biconvex profile, which is a very simple shape to make, is superior to the aerofoil at Mach numbers above 0·75, and that the circular-arc camber-line is on the whole superior to the parabolic-arc. The ' plate ' blades with blunt leading and trailing edges are poor in performance, but the ' plate with sharpened edges ' is reasonably good. It is suggested that very thin blades of the ' plate ' type may have certain applications.

1. *Introduction.*—Up to the present time, axial compressors for gas turbine units have always had blades of good aerodynamic design as a first requirement for high overall efficiency. This type of blade is comparatively difficult and costly to manufacture so that in the interests of speed and economy of production of certain types of axial compressor it may be found advantageous to sacrifice aerodynamic performance to some extent. An example of such an application is the engine of a guided projectile which is not reclaimable after its first useful flight.

The blades investigated were of such a profile that they could be made by simple turning or planing operations, and these were compared with two aerofoil cascades of similar geometric design.

Tests were made on No. 4 High-Speed Cascade Wind Tunnel and the comparison in performance was based on total-head loss, pressure rise, and deflection of the air in passing through the cascade. A full range of incidence and Mach number was covered from negative to positive stall condition, and up to choking Mach number.

α_1 range 40 deg to 70 deg

M range 0·1 to 1·0.

* N.G.T.E. Report No. R.60, received 22nd June, 1950.

2. *Description of Cascades.*—A standard nomenclature is used to describe normal cascade blades, giving in the following order, the blade thickness as a percentage of chord, profile shape, camber angle and the camber-line shape. For example:

10C4/25P40	10	maximum thickness of 10 per cent of the chord.
	C4	base profile is standard C4.
	25	camber angle is 25 deg.
	P40	camber-line is parabolic with its maximum distance from the chord-line 40 per cent of the chord from the leading edge.

This nomenclature gives the blade shape only and additional information is required to describe a cascade made up of such blades. This information is given in the table below:

Cascade type	Nomenclature	s/c	Chord in.	$-\zeta$	Throat / Pitch	β_2 deg	β_1 deg
1. Aerofoil (1)	10C4/25C50	0·75	1·30	42·5	0·585	30	55
2. Aerofoil (2)	10C4/25P40	0·75	1·30	37·6	0·648	30	55
3. Constant thickness (1) ..	7·2CT/25C50	0·75	1·30	42·5	0·576	30	55
4. Constant thickness (2) ..	7·2CT/25P40	0·75	1·30	37·6	0·650	30	55
5. Sharpened constant thickness	8·5CT(S)/25C50	0·75	1·30	42·5	0·605	30	55
6. Two arc	10·5/2A/25C50	0·75	1·30	42·5	0·588	30	55

It will be noticed that the cascades all have the same blade angles, pitch/chord ratio, and chord, and are therefore termed geometrically similar cascades.

The CT and 2A codes used in the table were invented to fit into the standard form, but these obviously do not describe the blades fully; leading and trailing-edge radii of the unconventional blades together with other details are shown in Fig. 2. The thickness ratio of the blades is so arranged that they have constant sectional area.

A cascade is made up of eight blades fixed rigidly between side walls by means of three pin supports at the ends of each blade. At the cascade ends are boundary-layer bleed chambers with the bleed slit formed between the extreme blades and the bottom face of the chamber. The whole cascade is made of an aluminium bronze which is easy to work and cast.

3. *Description of the Wind Tunnel.*—The wind tunnel itself consists of wooden feed sections highly polished on their inner surfaces, on the end of which the cascade is bolted. Each feed piece corresponds to a definite gas inlet angle and these were chosen to give a range from 40 deg to 70 deg at $2\frac{1}{2}$ deg intervals.

The air supply for the wind tunnel is fed through a settling chamber containing gauzes, then contracts into the wind tunnel at an area ratio of about 20: 1 and exhausts from the cascade into free air, no side wall extensions being used. Provision is made for removing boundary layers, by bleed chambers connected to the suction trunking of the laboratory. By these means an almost flat velocity profile is produced at entry to the cascade and the results obtained are very nearly two-dimensional.

3.1. *Instrumentation.*—Pressure measurements made in the wind tunnel before the air reaches the cascade are, upstream total head, measured in the settling chamber and upstream static pressure measured by ten static-tubes, five equi-spaced on each side wall and about one chord upstream of the cascade. The traverse instrument mounting is shown in Fig. 1 and incorporates a pendulum inclinometer by which the angle of turn of the claw-type yawmeter is read against a pendulum controlled datum line.

All pressures are measured on a manometer in which all the tubes are duplicated in water and mercury so that the approximately 100: 1 pressure range required for a 10: 1 velocity range can be obtained. When pressures reach the limit of water-tube measurement these are isolated by simply clamping the rubber connecting tubes.

4. *Test Procedure.*—Most of the test procedure is concerned with gas angle measurement and is in effect a calibration of the yawmeter and wind-tunnel end.

Before testing each cascade, an open wind-tunnel traverse is made along the wind-tunnel centre-line from each side of the tunnel end, thus giving the efflux angle of the air relative to the datum line. The datum line itself is pendulum controlled so that the gas angle is known relative to the vertical. If the angle of the face upon which the cascade is placed is measured relative to the horizontal with a bubble-type inclinometer, then the absolute value of the air inlet angle is known. This method of finding the gas inlet angle eliminates two possible sources of error :

(*a*) The assumption that the air approaches the cascade in a direction parallel to the wind-tunnel walls.

(*b*) Movement of the traverse gear mounting during test.

The only likely source of error remaining is that produced by damage or interference with the yawmeter claws. This is guarded against by checking one open wind-tunnel traverse at the end of the tests for a single incidence.

The traverse when the cascade is in position is made over the wakes of two blades on the cascade centre-line, readings being taken at 1/60th in. intervals where necessary. The mean of the total-head loss and deflection over these two pitches are the quantities taken as indicative of the cascade performance at the particular incidences. Before each test with the cascade in position is started, the boundary-layer bleed must be adjusted by regulating the bled mass flow from each end of the cascade so that the ten upstream static-tubes read pressures which are as nearly as possible equal.

4.1. *Cascade Inspection.*—When a cascade is manufactured it is inspected to see that certain dimensions called for on the drawing are within the prescribed limits. Unfortunately the cascades were not projected before the tests began, but the result of projecting the profiles at the end of the tests is shown in the table below where manufacturing errors are recorded.

In this table the numbers 4, 5 and letter D refer to the two blades traversed and the blade called for in the drawing, respectively.

Cascade Accuracy

Blade	Stagger ($-\zeta$)			L.E. Radius			T.E. Radius			Chord		
	4	5	D	4	5	D %	4	5	D %	4	5	D
10C4/25C50 ..	42·4	42·3	42·5	—	10	12	—	4·2	6	—	1·298	1·3
10C4/25P40 ..	37·9	37·5	37·6	—	17	12	—	6·2	6	—	1·298	1·3
7·2CT/25C50 ..	42·2	42·4	42·5	52	51	50	52	52	50	1·294	1·295	1·3
7·2CT/25P40 ..	37·7	37·6	37·6	48	48	50	48	48	50	1·300	1·300	1·3
8·5CT(S)/25C50 ..	42·2	42·1	42·5	4·5	4·6	5	4·2	5·2	5	1·300	1·298	1·3
10·5/2A/25C50 ..	42·0	41·9	42·5	4·8	7·3	5	4·0	5·5	5	1·298	1·295	1·3

From the above, it is evident that the only factors which may possibly affect the blade performance are the leading-edge radii of the first two and last blades. The C4/C50 has a sharper nose than a correct C4 profile and the C4/P40 and 2A/C50 have noses more rounded than the design value.

The last two cascades have comparatively large errors in stagger angle which are taken into account when deviation values are calculated.

5. *Presentation of Results.*—The results of the tests are plotted in three ways, each having some advantage for comparison purposes. The three methods are :

(*a*) Loss coefficient and deflection against inlet angle $\frac{\bar{\omega}}{\frac{1}{2}\rho V_1^2}$, ε against α_1.

(*b*) Maximum L/D ratio, C_L at maximum L/D and C_L at stall, all against entry Mach number.

(*c*) Characteristic curves.

The first two methods are well known, $\bar{\omega}/\frac{1}{2}\rho V_1^2$ and ε being the measurement obtained directly from the wind tunnel and C_L and C_{Dp} being defined as:

$$C_L = 2\,s/c\,(\tan\alpha_1 - \tan\alpha_2)\cos\alpha_m - C_D\tan\alpha_m$$

$$C_{Dp} = s/c\,.\,\bar{\omega}/\tfrac{1}{2}\rho V_1^2 \times \cos^3\alpha_m/\cos^2\alpha_1.$$

Method (*c*) needs some explanation, but is considered by the author to be most instructive in performance comparison, especially where the running conditions to be used are at a high Mach number. The method is to consider the cascade as a single blade row in which half the work done by the row appears as kinetic energy; this gives rise to the same condition as in a 50 per cent reaction stage, *i.e.*, $\tan\alpha_0 = \tan\alpha_2 = \tan\alpha_4$. The blade speed is thus fixed relative to the inlet velocity or Mach number, then assuming the axial velocity through the blade row is constant, the temperature rise or work done can be expressed in terms of the inlet Mach number

$$\frac{\Delta T}{T_1} = \frac{\gamma - 1}{2} M_1^2 \left(1 - \frac{\cos^2\alpha_1}{\cos^2\alpha_2}\right).$$

Also for the efficiency calculation, if P_2' is the static pressure after the cascade with no losses

$$P_2 = P_2' - \bar{\omega}$$

and we define

$$\eta = \frac{\Delta T_{ad}}{\Delta T} = \frac{\left(\frac{P_2' - \bar{\omega}}{P_1}\right)^{\frac{\gamma-1}{\gamma}} - 1}{\Delta T/T_1}.$$

Or in terms of measured quantities

$$\eta = \frac{\left\{\left[1 + M_1^2\frac{(\gamma-1)}{2}\left(1 - \frac{\cos^2\alpha_1}{\cos^2\alpha_2}\right)\right]^{\frac{\gamma}{\gamma-1}} - \frac{\bar{\omega}}{P_{tot} - P_1}\left[\left(1 + \frac{\gamma-1}{2}M_1^2\right)^{\frac{\gamma}{\gamma-1}} - 1\right]\right\}^{\frac{\gamma-1}{\gamma}} - 1}{M_1^2\frac{(\gamma-1)}{2}\left(1 - \frac{\cos^2\alpha_1}{\cos^2\alpha_2}\right)}.$$

This formula gives efficiencies 0·1 to 0·2 per cent greater than those given by the formula

$$\eta = 1 - \frac{\bar{\omega}}{(P_{tot} - P_1)\left(1 - \frac{\cos^2\alpha_1}{\cos^2\alpha_2}\right)}$$

which is the incompressible form, for loss coefficients of the order of 0·02 to 0·03.

Thus, temperature rise and efficiency can be obtained at all incidences for each inlet Mach number and if these quantities are plotted against axial Mach number $M\cos\alpha_1$, a series of characteristics is obtained, each curve corresponding to one inlet Mach number. It must be remembered, however, that the high half-stage efficiencies are due to considering two-dimensional losses only.

Also plotted are the maximum and criticial Mach numbers for each cascade. Maximum Mach number at a given incidence is said to be that at which the measured pressure rise is zero, and the critical Mach number that at which the loss is 1·5 times its minimum value.

6. *Discussion of Results.*—There are two possible comparisons to be made from the cascades tested, the first that of camber-line shape from the aerofoil and constant thickness blades, and secondly that of profile shape on blades of otherwise identical geometrical properties. In the

following sections standard nomenclature rather than verbal description will be used to describe the blades, in order to prevent confusion. Thus the cascades are:

(*a*) C4/C50 standard aerofoil/circular camber-line.

(*b*) C4/P40 standard aerofoil/parabolic camber-line.

(*c*) CT/C50 constant thickness/circular camber-line.

(*d*) CT/P40 constant thickness/parabolic camber-line.

(*e*) CT(S)/C50 constant thickness, sharpened/circular camber-line.

(*f*) 2A/C50 two circular-arcs/circular camber-line.

6.1. *Effect of Camber-Line* (P40 *against* C50).—The change in camber-line is one of change in position of maximum camber from the centre of the chord-line to a position 40 per cent of the chord from the leading edge. This change produces a higher curvature at the leading edge, and correspondingly lower at the trailing edge. The change also gives a larger throat area, and the expected performance for a P40 camber-line blade is therefore: lower deviations because of the longer blade tail, lower critical Mach number due to higher curvature at the forward top surface, and higher maximum Mach number at inlet because of the larger throat.

The two outstanding features of the CT (constant thickness) cascades, Figs. 7 to 10, are first the shift of minimum loss incidence from about — 3 deg in the case of the CT/P40, to + 2 deg in the case of the CT/C50, and the steep fall off in CT/C50 deflection with decrease of incidence. For both cascades the same general shape of deflection curve is maintained throughout the speed range, with apparently little Reynolds number effect; there is, however, a rise in loss with Mach number which is steeper for the CT/C50 blade, due to its smaller throat width. The minimum loss of the CT/P40 blade is somewhat lower than that for the CT/C50 at $M = 0{\cdot}4$ but has the disadvantage that it is at a 5 deg lower incidence and deflection than the latter blade and is therefore less useful.

A similar state of affairs exists between the C4/P40 and C4/C50 blades, Figs. 3 to 6, the low loss incidence range for the C4/P40 is again 5 deg lower than for the C4/C50. The excessive fall off in deflection with decreased incidence is not evident in C4/C50 curve as the aerofoil form of the C4 profile tends to keep the minimum pressure point well forward. There is a quite similar fall in deflection at higher Mach numbers, due however to shock formation and not pressure gradient. The extra incidence that the C4/C50 will take gives it a value of maximum deflection which is 3 or 4 deg higher than that for the C4/P40 thus giving it a higher possible work capacity as a compressor blade row, other things being equal.

But for the 5 deg shift of incidence, the curves for the two blades C4/P40 and C4/C50 are quite similar as regards Mach number and Reynolds number effect. The differences are: rather more fall off in performance at low Reynolds number for the C4/C50 blade and a negative incidence stall for the blade at high Mach numbers which has already been mentioned. There is not much difference between the minimum losses of the two cascades, but the combined effect of loss and deflection can be seen as the characteristic curves (Fig. 17). From these curves it is obvious that the C4/C50 blade has a greater working range at high efficiency, and a greater work capacity, particularly at high Mach number.

There is not much to be learnt from the CT/C50 and P40 critical Mach number curves as the minimum loss is so high that the 1·5 minimum loss does not bear the same relation to Mach number as in the normal low loss aerofoil case. The maximum Mach number curves for the two CT cascades fall off at high incidence due to the high losses which reduce the pressure rise.

The critical Mach number of C4/P40 is lower than that for the C4/C50 because of its higher top-surface suction, but the choking mass flow is greater in the ratio of the throat areas, *i.e.*, 0·90.

6.2. *Comparison of* C4/P40 *and* C4/C50 *with previous Results* (*Figs.* 3 *to* 6).—The minimum loss coefficient of 0·016 for the two cascades is about equal to the minimum loss for similar cascades given in Refs. 1, 3 and 5. In Ref. 1 also, is an example of the working range shift towards lower incidence for the P40 blades.

The maximum deflection attained by the C4/P40 cascade is about 0·5 deg higher than that predicted in Ref. 6, p. 445, but the C4/C50 maximum deflection at 0·4 Mach number is 4·5 deg higher than this predicted value (*see* section 8.0).

Some high-speed tests on circular-arc cambered cascades at Mach number 0·6 (Ref. 5) give very low deflection even when an allowance (about 3 deg) is made for the high s/c. However, the loss curve interpolated from these results (Fig. 4) shows that the results are compatible.

In Ref. 4 the critical Mach number has been predicted for a cascade (11C2/25P47) of comparable camber by the von Kármán formula. The curve has two branches corresponding to the critical point being in the bottom and top surfaces respectively. The top-surface part of the curve agrees well with the curve for the C4/P40, C4/C50, but the bottom-surface branch is much lower than the test results, probably because of the higher s/c of the C2/P47 cascade.

The maximum and critical Mach numbers of a 7·5C1/25C50 as interpolated from Ref. 5 agree well with the results for the C4/C50 cascade, although the critical Mach number criterion was different in the two cases. For the C4/C50, P40 cascades critical Mach number is said to be that where the loss coefficient rises to 1·5 times its minimum value, and for the cascade in Ref. 5 a fall in the pressure-rise curves is taken to denote critical conditions, all measurements being at constant incidence.

6.3. *Effect of Blade Profile.*—In this section the cascades considered will be of the circular-arc camber-line type, with varying profile shapes :

(*a*) 10C4/25C50	or C4/C50	(Symbol used in text)
(*b*) 7·2CT/25C50	or CT/C50	(Symbol used in text)
(*c*) 8·5CT(S)/25C50	or CT(S)/C50	(Symbol used in text)
(*d*) 10·5/2A/25C50	or 2A/C50	(Symbol used in text) .

7·2CT/25C50 (Figs. 7 and 8).—Because of its thick trailing edge, the minimum loss of the CT/C50 cascade is too high at any speed to be of use in almost any application. In addition to its high loss the incidence range is very poor being only about one third that for the C4/C50, a surprising fact considering the rounded nose of the CT/C50. The effect of Mach number is to produce a loss increase over the whole incidence range with a corresponding fall in deflection; there is no incidence at which the loss remains invariable with Mach number as in the C4/C50 cascade. The fact that the deflection and loss curves are in such a uniform family indicates that increase in Mach number produces only a worsening of the flow conditions, with no definite change in flow configuration such as would be produced by shock-waves at say, $M = 0{\cdot}8$. On the other hand the C4/C50 blade is shock-stalled for low and high incidence at Mach number 0·8 and this blade has a relatively sharper nose.

The performance curves of the cascade (Fig. 18) show well the poorness, in every respect, of the CT/C50 cascade relative to the C4/C50 at all speeds.

It is the thickness of the CT/C50 which makes it so poor and if a thin blade were used in, for instance, a low-speed fan, where stresses are not high, a flat plate might have a much improved performance. Comparing two isolated aerofoils (Fig. 22), one a flat plate of 2·1 per cent thickness[8] and the other an aerofoil approximately P40 (Ref. 9, p. 42) of 10 per cent thickness ratio, the performance of the flat plate is as good as that of the aerofoil. On these curves also are plotted C_L and C_{Dp} of the similar cascade blades as a comparison of curve shape. The CT/C50 cascade and the constant thickness isolated blade have quite similar loss and deflection curves.

8·5CT(S)/25C50 (Figs. 11 and 12).—This blade profile can be considered as a CT/C50 blade sharpened at leading and trailing edges, in which case the sharp trailing edge should eliminate the large wake loss, and the leading edge should give favourable Mach number characteristics and unfavourable incidence characteristics. The first two effects are as expected, but the incidence range at low loss is comparatively high because the deterioration of performance at high incidence is gradual, leading to a gentle rise in loss coefficient and a fall in slope of the deflection curve.

The Mach number effects at 0 deg incidence are small as expected till a value of 0·8 is reached when the minimum loss begins to increase. The maximum deflection decreases continuously from the lowest Mach number to the highest owing probably to the high velocities induced and the small leading-edge radius. One unique point in these curves is that of $\alpha_1 = 65$ deg at $M = 0{\cdot}8$; here the loss falls and the deflection rises suddenly, indicating a favourable shock formation in the blade passages, producing shock compression. The effect of this can be seen on the performance curves (Fig. 18) in the form of a temporary increase in efficiency with decreasing axial Mach number on the $M = 0{\cdot}8$ characteristic.

10·5/2A/25C50 (Figs. 13 and 14).—Unlike the previous cascade the 2A/C50 has a minimum loss at low speeds which is as low as that for the C4/C50 and although the range of incidence for low loss decreases with Mach number the value of minimum loss at a particular Mach number does not increase a great deal as the Mach number increases. Above $M = 0{\cdot}4$ the value of deflection at 0 deg incidence increases so that net effect of loss and deflection on the performance curve (Fig. 19) is to give the widest range at high efficiency at $M = 0{\cdot}7$ compared with a value of $M = 0{\cdot}5$ or below for the other cascades.

The highest efficiency attained by any of the cascades is between 96 and 97 per cent and this efficiency is maintained by the 2A/C50 cascade up to a Mach number of 0·78. Thus from the point of view of high pressure rise per stage at high efficiency the 2A/C50 is superior to the C4/C50 except for its slightly smaller range. At lower speeds, however, the C4/C50 has the advantage of a much wider range and a higher possible pressure rise, due to its higher maximum deflection.

The superiority of a normal aerofoil (11C2/40C50) over a two-arc blade shape at low speed is shown in Ref. 1. Here the reduction in maximum deflection is just as great as between the C4/C50 and 2A/C50 and the two-arc blade has a very restricted low-loss range. The fact that the two-arc blade is, in this respect, relatively worse than the 11C2/40C50 as compared with the C4/C50 and 2A/C50 is due probably to the high camber and pitch/chord ratio.

From a comparison of the performance of two isolated aerofoils, Fig. 22, one with a flat under surface and a circular-arc top surface (R. & M. 2301[7]), the other aerofoil shape roughly P40 parabolic[9], it is evident that at low Mach numbers a two-arc blade can have as low a loss as an aerofoil but usually suffers through early stalling. In R. & M. 2301[7], the effect of leading-edge radius in an isolated aerofoil of 10 per cent thickness ratio is also discussed and very little difference is produced in $C_{L\max}$ and $C_{D\min}$ at $Re = 3 \times 10^5$.

The performance characteristics (Fig. 19) show well the flattening of the temperature-rise curves due to early but gradual stall; also the wide high efficiency range at high Mach numbers, in contrast to the C4/C50 cascade. The maximum pressure rise at a given speed is below the value for the C4/C50 at every Mach number except 0·8 where the pressure rise, already higher than that for the C4/C50 is increased due to shock compression with a temporary increase in efficiency.

7. *Reynolds Number Effects.*—The three constant-thickness cascades have no serious deterioration in performance at even the lowest test Reynolds number except for a two-degree drop in deflection in the CT(S)/C50 at negative incidences.

For the remainder, performance begins to deteriorate at about $Re = 1{\cdot}7 \times 10^5$ (no turbulence factor allowance) and from this speed down to $Re = 0{\cdot}8 \times 10^5$, there is a drop in deflection and increase in loss varying in character with the cascade. Both the C4/C50 and 2A/C50 have a

general decrease in deflection over the whole incidence range, 2 to 5 deg in the former case and about 7 deg in the latter. The C4/P40 on the other hand, remains unaffected at low incidences but the stalling incidence is seriously reduced.

8. *General Numerical Comparison.*—The following table gives in brief some of the main properties of the cascades here reported and those reported in the references. Results refer in the main to low-speed incompressible performance, $M = 0{\cdot}4$ being taken as the best speed for the five cascades tested.

Cascade	Stagger ζ	s/c	δ^*	ε^*	$C_{L\,max}$	$C_{D\,min}$
10C4/25P40 ($M = 0{\cdot}4$)	−37·6	0·75	4·4	21·0	1·03	0·016
10C4/25C50 ($M = 0{\cdot}4$)	−42·5	0·75	6·0	24·4	1·28	0·018
7·2CT/25P40 ($M = 0{\cdot}4$)	−37·6	0·75	4·1	20·0	0·70	0·050
7·2CT/25C50 ($M = 0{\cdot}4$)	−42·5	0·75	7·3	18·2	0·82	0·055
8·5CT(S)/25C50 ($M = 0{\cdot}4$)	−42·5	0·75	9·9	16·3	0·83	0·020
10·5/2A/25C50 ($M = 0{\cdot}4$)	−42·5	0·75		18·2	0·89	0·017
11/2A/40C50 Ref. 1	−27·5	0·94	9·8	27·5	1·12	0·016
11C2/40C50 Ref. 1	−27·5	0·94	8·5	26·1	1·35	0·018
RAF27/5C50 Ref. 3	−27·4	0·75	4·0	20·0	0·80	0·019
Isolated Aerofoils	—	—	—	—	$C_{L\,max}$	$C_{D\,min}$
($Re = 3{\cdot}0 \times 10^5$)						
102A/23C50 Ref. 7	—	—	—	—	1·07	0·022
2·1CT/25C50 Ref. 8	—	—	—	—	1·32	0·018
10/G450/28P40 Ref. 9	—	—	—	—	1·29	0·023
Rules, etc.	Stagger ζ	s/c	δ^*	ε^*	—	—
Deviation Rule (P40) Ref. 2	−37·6	0·75	4·8	—	—	—
Deviation Rule (C50) Ref. 2	−42·5	0·75	6·4	—	—	—
Ref. 6, pp. 445 to 446 (P40)	−37·6	0·75	4·7	20·5	—	—
Ref. 6, pp. 445 to 446 (C50)	−42·5	0·75	6·5	20·5	—	—

9. *Conclusions.*—The 10C4/25P40 cascade has a working range at low loss about equal to the 10C4/25C50 but this range for the latter cascade is at an incidence and therefore deflection 3 to 5 deg higher than for the C4/P40 thus giving the C4/C50 a higher work capacity. The high Mach number characteristics of the C4/C50 are rather better than for the C4/P40 although this cascade has the larger throat and therefore largest choking flow.

The difference in performance between cascades is predictable in terms of the higher top-surface suction peak existing on the C4/P40 blades and to some extent the rather sharper nose shape of the C4/C50. Relative to design rules given in Refs. 1 and 6, the C4/P40 results are as expected and the C4/C50 better than expected.

The performance of the 7·2CT/25P40 and the 7·2CT/25C50 bear the same relation to one another as the C4/P40 and C4/C50 but as individual cascades their performance is bad, having a high minimum loss due to the thickness of the trailing edge and the adverse effects of the profile on the pressure distribution. Such a cascade as this could only be of use if the thickness/chord ratio were reduced when, from isolated aerofoil tests, the performance could be expected to improve considerably. An improvement could also be made by sharpening the trailing edge.

The 8·5CT(S)/25C50 cascade suffers through having a low maximum deflection and relatively high minimum loss so that its showing on the performance curve is indifferent. The working range is fairly wide, but the drop in efficiency is sudden when stalled condition is reached and the

maximum value of efficiency obtained is 3 per cent lower than for the C4/C50 or 2A/C50. The poorness of the cascade is probably due to the discontinuities of the blade surface especially on the trailing top surface, and when these are removed, as effectively they are, for the 2A/C50, an improvement in performance is obtained.

The 10·5/2A/25C50 has a somewhat low stalling deflection at low speeds, but at high speeds, M 0·7 to 0·8, the cascade has a general performance superior to the C4/C50. This cascade obviously has possibilities for high-speed application.

Acknowledgment.—The author is indebted to Mrs. M. Smith and Mrs. P. M. Andrews for carrying out the majority of the laborious traversing and initial plotting work.

REFERENCES

No.	*Author*	*Title, etc.*
1	A. R. Howell	Note on Compressor Base Aerofoils C.1, C.2, C.3, C.4, C.5 and Aerofoils made up of Circular Arcs. Power Jets Memorandum M.1011.
2	A. D. S. Carter and Hazel P. Hughes ..	A Theoretical Investigation into the Effect of Profile Shape on the Performance of Aerofoils in Cascade. R. & M. 2384. March, 1946.
3	H. Constant	Performance of Cascades of Aerofoils. R.A.E. Note E.3696.
4	A. R. Howell	Present Basis of Axial Flow Compressor Design. Part I. A.R.C. 4155.
5	F/Lt. Bailey and J. L. Jefferson	Compressibility Effect on Cascades of Low Cambered Compressor Blades. A.R.C. 6955.
6	A. R. Howell	Fluid Dynamics of Axial Compressors. *Proc. Inst. Mech. Engr.* 1945. Vol. 153, p. 441 (War Emergency Issue No. 12).
7	D. H. Williams, A. F. Brown and C. J. W. Miles	Tests on Four Circular-Back Aerofoils in the Compressed Air Tunnel. R. & M. 2301. June, 1946.
8	R. A. Wallis	Wind-Tunnel Tests on a Series of Circular-Arc Plate Aerofoils. Aerodynamic Note No. 47, Australian Council for Scientific and Industrial Research, Division of Aeronautics.
9	A. Betz	Applied Aerofoil Theory. W. F. Durand's, *Aerodynamic Theory*. Division J, Chapter II. Section 6.

NOTATION

C	Chord
S	Pitch
θ	Camber
ζ	Stagger
t/c	Thickness ratio
A_T	Throat area
A_I	Inlet area
β	Blade angle
α	Gas angle
α_m	Vector mean angle
ε	Air deflection angle
δ	Deviation
δ^*	Nominal deviation
$\bar{\omega}$	Mean total pressure loss
T_1	Static temperature at inlet to cascade
ΔT	Static temperature rise through cascade
ΔP	Static pressure rise through cascade
ΔT_{ad}	Adiabatic temperature rise through cascade
P	Static pressure
P_2'	Static pressure after cascade with no losses
P_{tot}	Total-head upstream pressure
P_a	Barometric pressure
C_L	Lift coefficient
C_L^*	Nominal lift coefficient $= 0{\cdot}8C_{L\,\max}$
C_{Dp}	Profile drag coefficient
Re	Reynolds number

Suffixes—

1	Cascade inlet
2	Cascade outlet

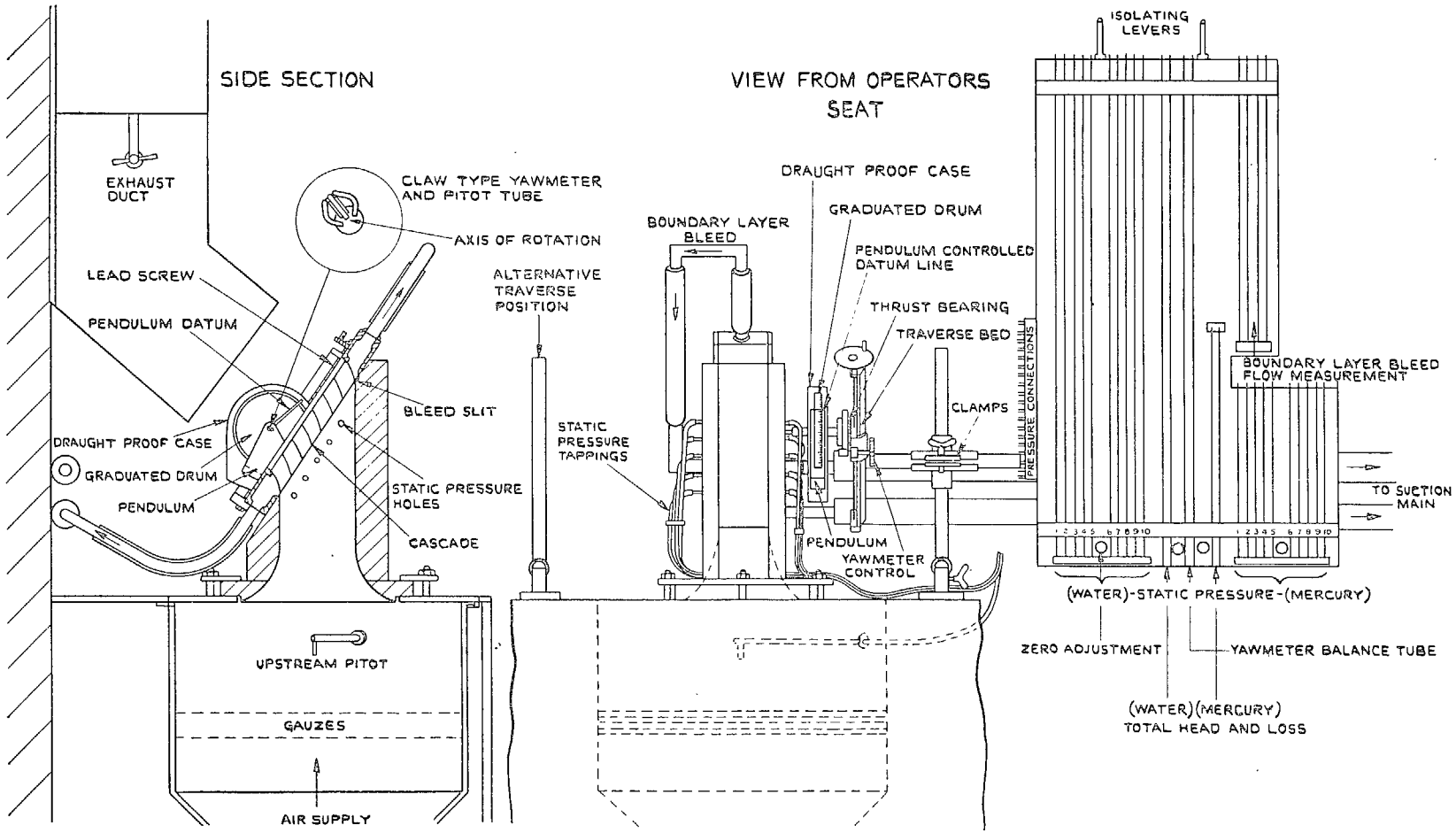

FIG. 1. Layout of No. 4 High-Speed Cascade Wind Tunnel.

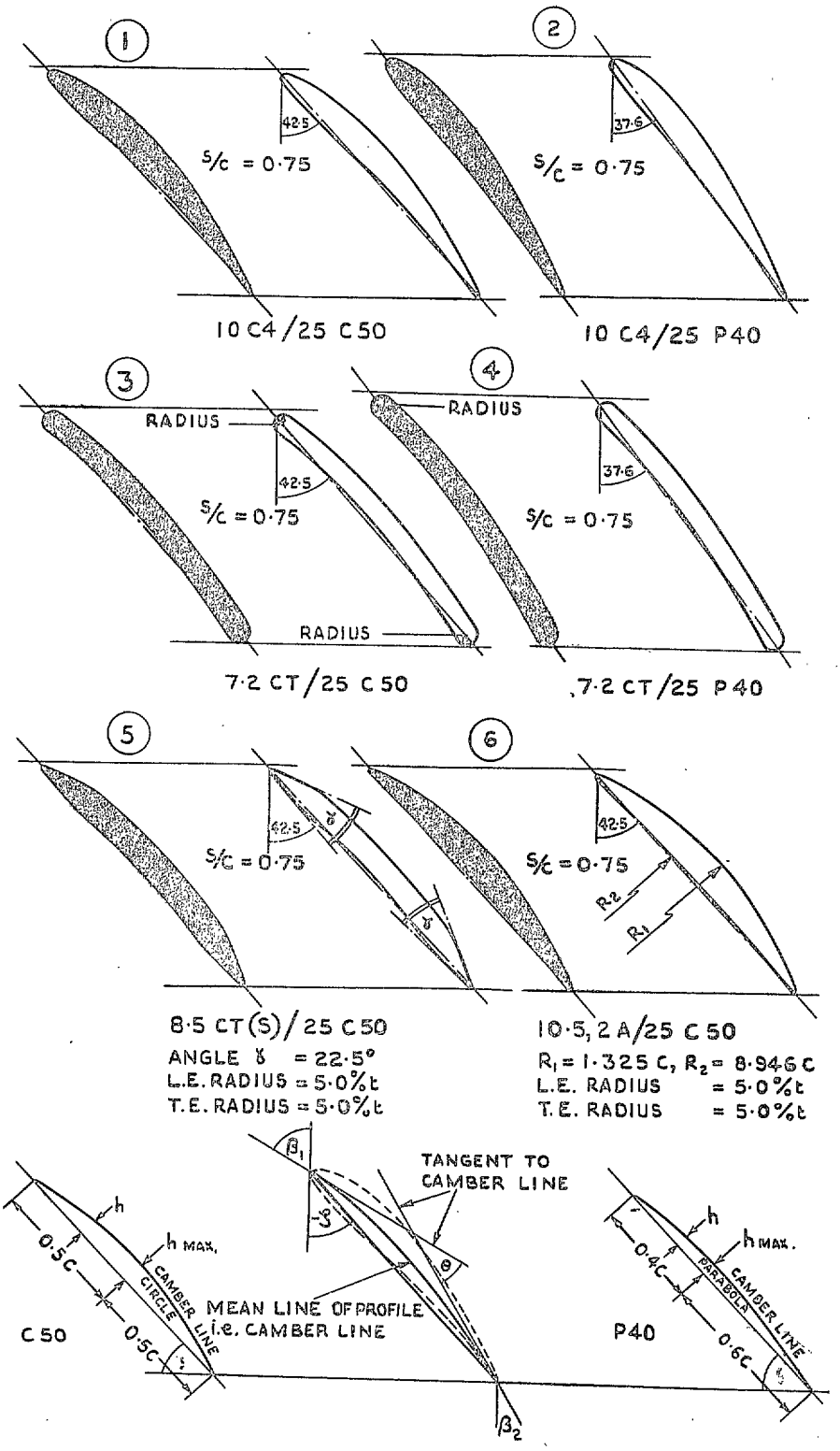

FIG. 2. Cascade data.

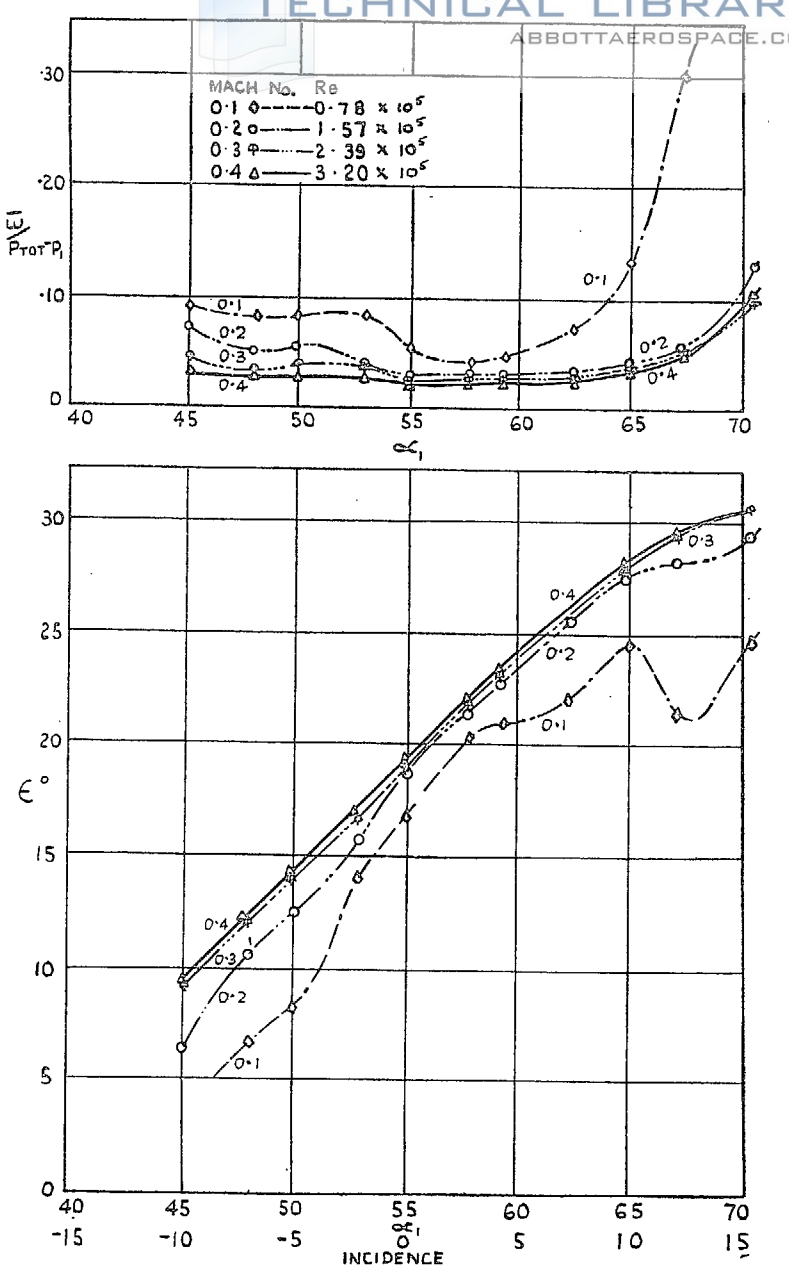

FIG. 3. Cascade 10C4/25P40.

$\frac{\bar{\omega}}{P_{tot}-P_1}$ and ε against α_1. Low Mach numbers.

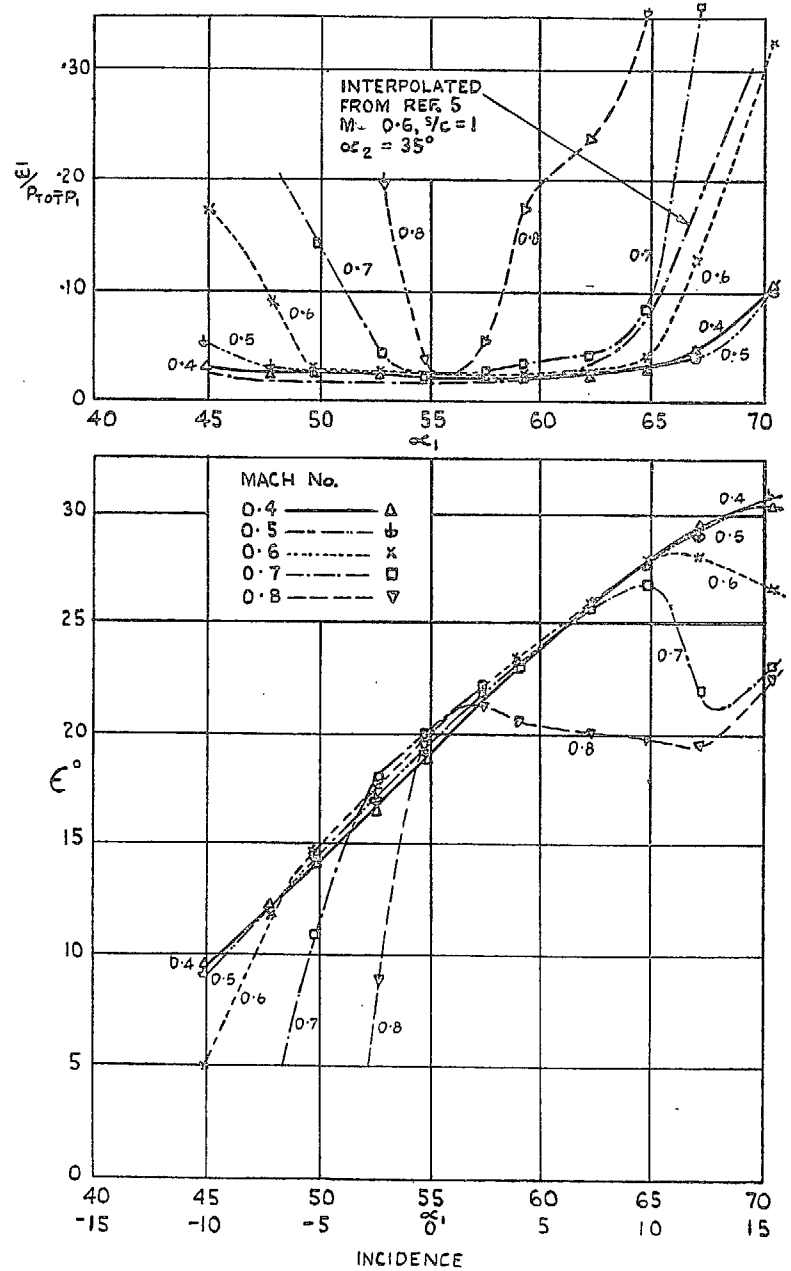

FIG. 4. Cascade 10C4/25C50.

$\frac{\bar{\omega}}{P_{tot}-P_1}$ and ε against α_1. High Mach numbers.

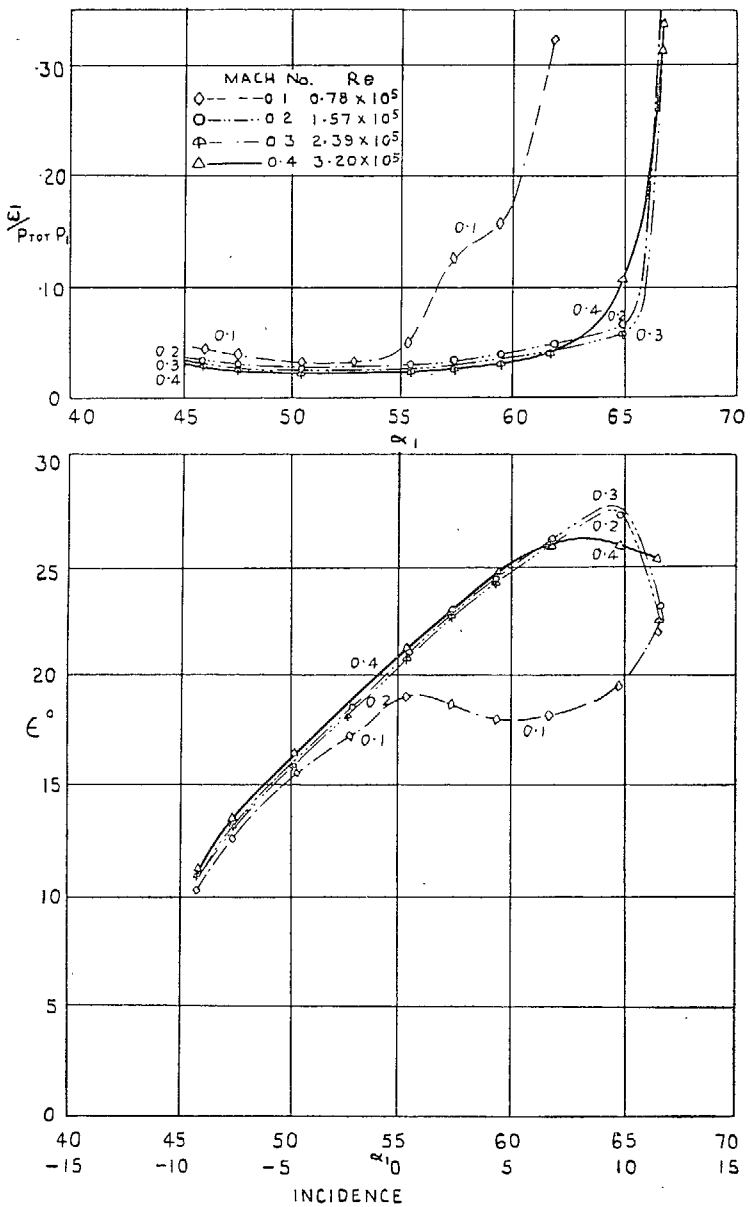

FIG. 5. Cascade 10C4/25P40.

$\frac{\bar{\omega}}{P_{tot} - P_1}$ and ε against α_1. Low Mach numbers.

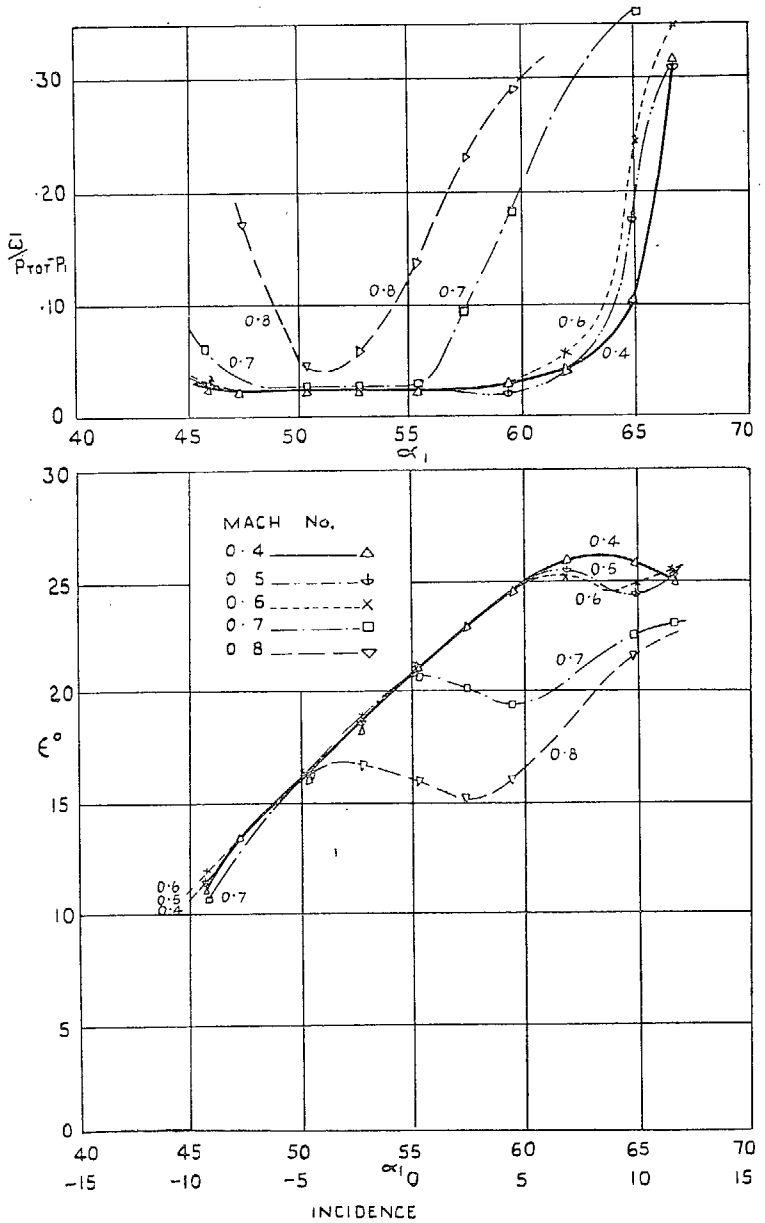

FIG. 6. Cascade 10C4/25P40.

$\frac{\bar{\omega}}{P_{tot} - P_1}$ and ε against α_1. High Mach numbers.

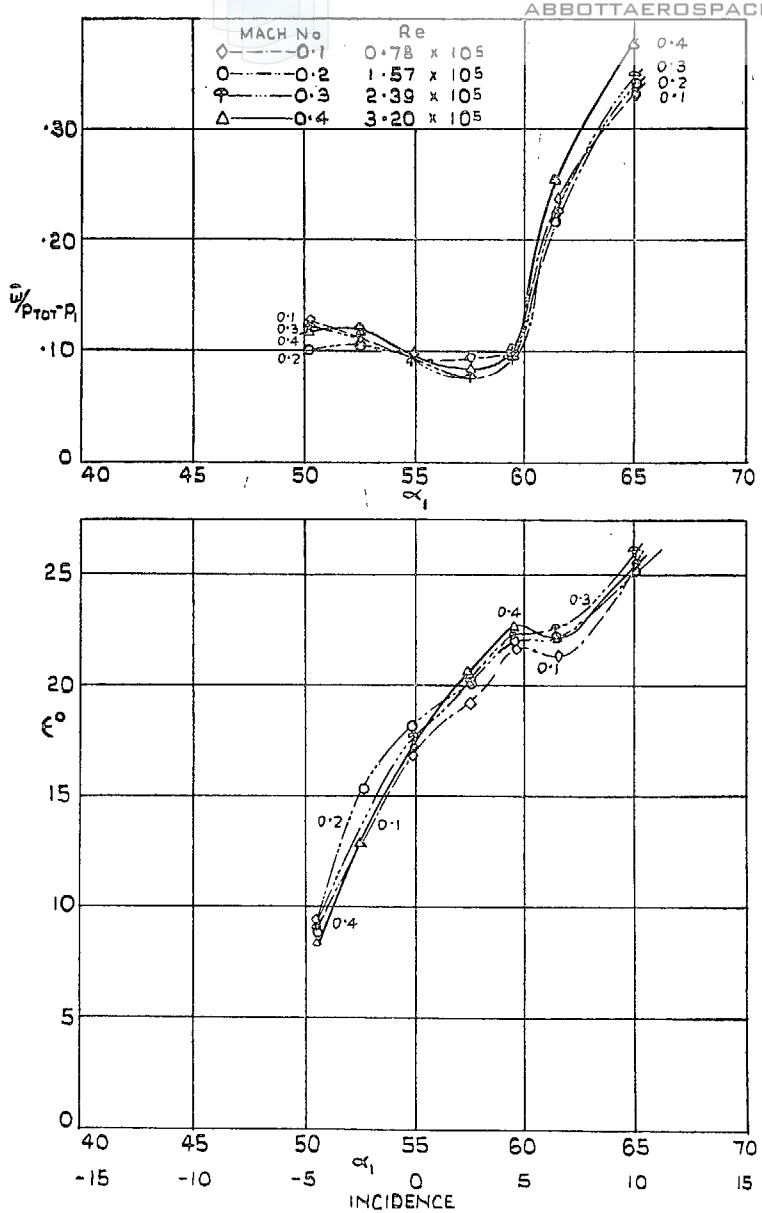

FIG. 7. Cascade 7·2CT/25C50.

$\frac{\bar{\omega}}{P_{tot} - P_1}$ and ε against α_1. Low Mach numbers.

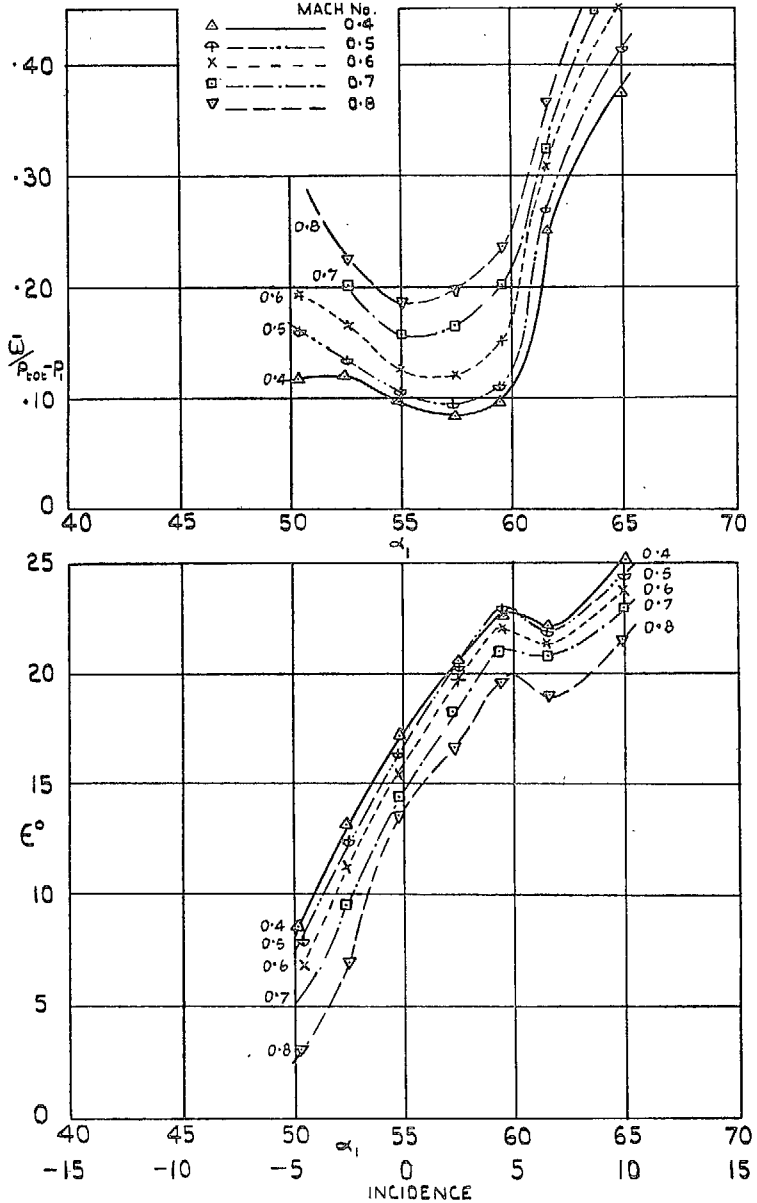

FIG. 8. Cascade 7·2CT/25C50.

$\frac{\bar{\omega}}{P_{tot} - P_1}$ and ε against α_1. High Mach numbers.

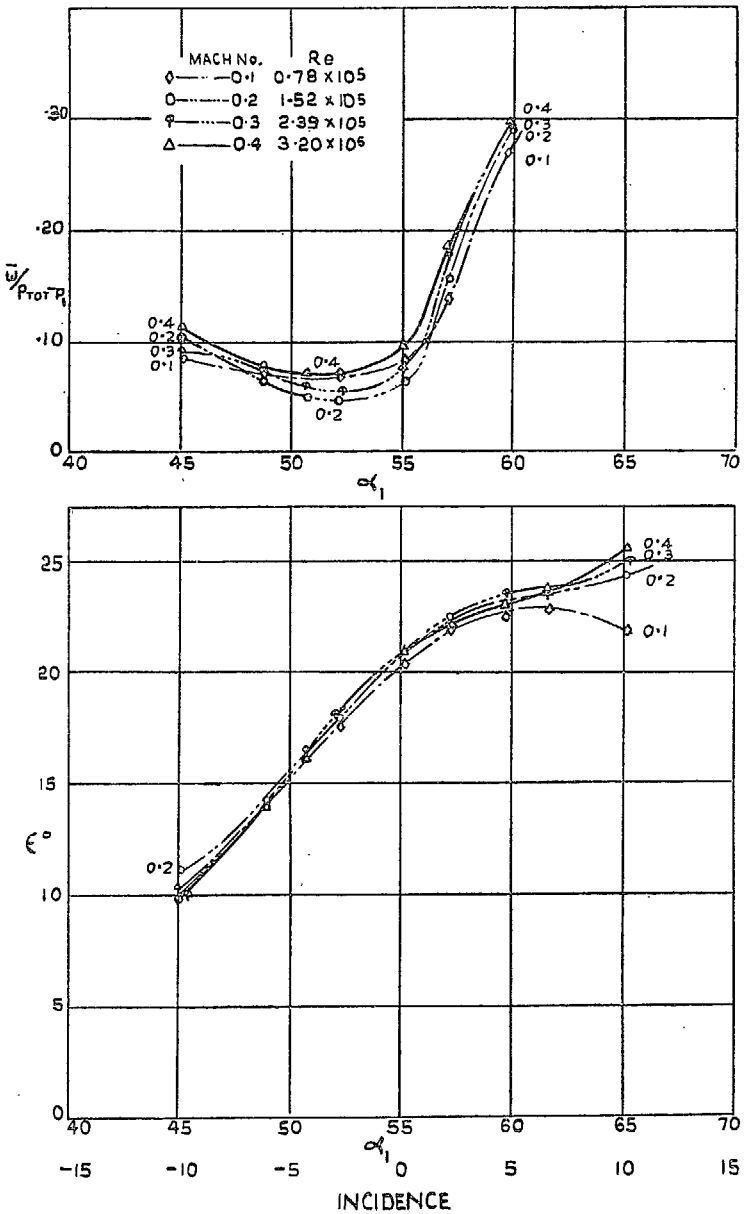

FIG. 9. Cascade 7·2CT/25P40.

$\frac{\bar{\omega}}{P_{tot} - P_1}$ and ε against α_1. Low Mach numbers.

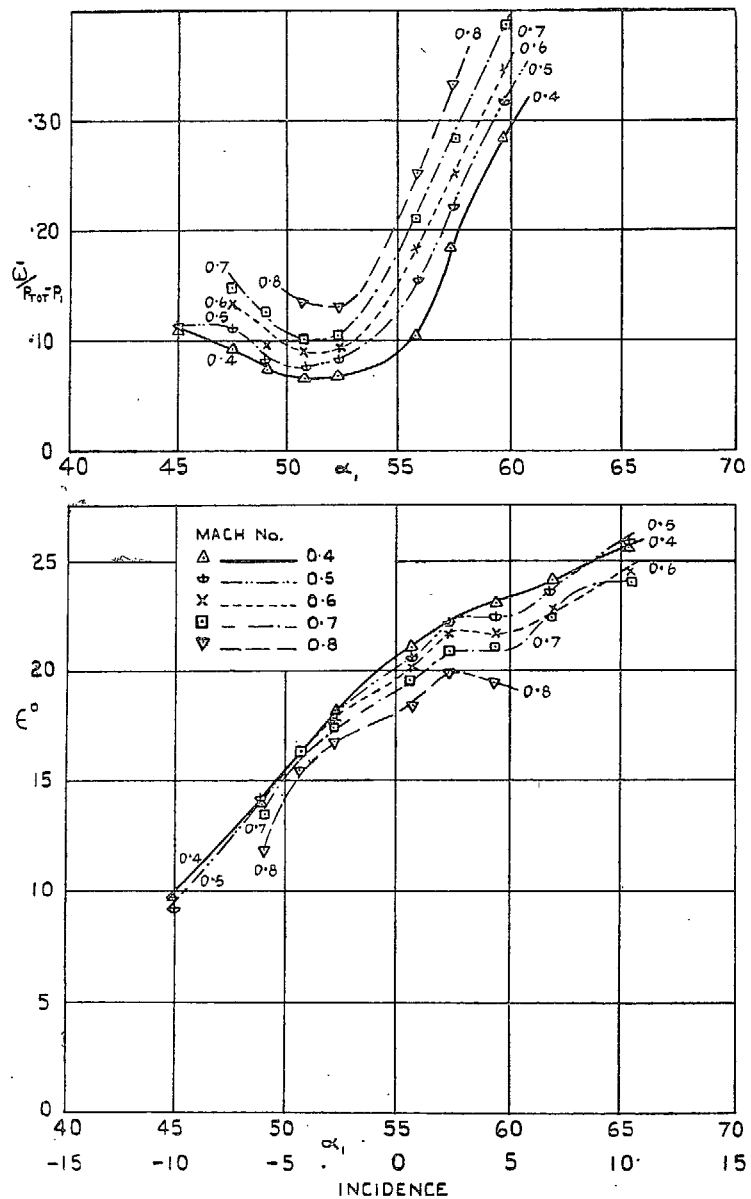

FIG. 10. Cascade 7·2CT/25P40.

$\frac{\bar{\omega}}{P_{tot} - P_1}$ and ε against α_1. High Mach numbers.

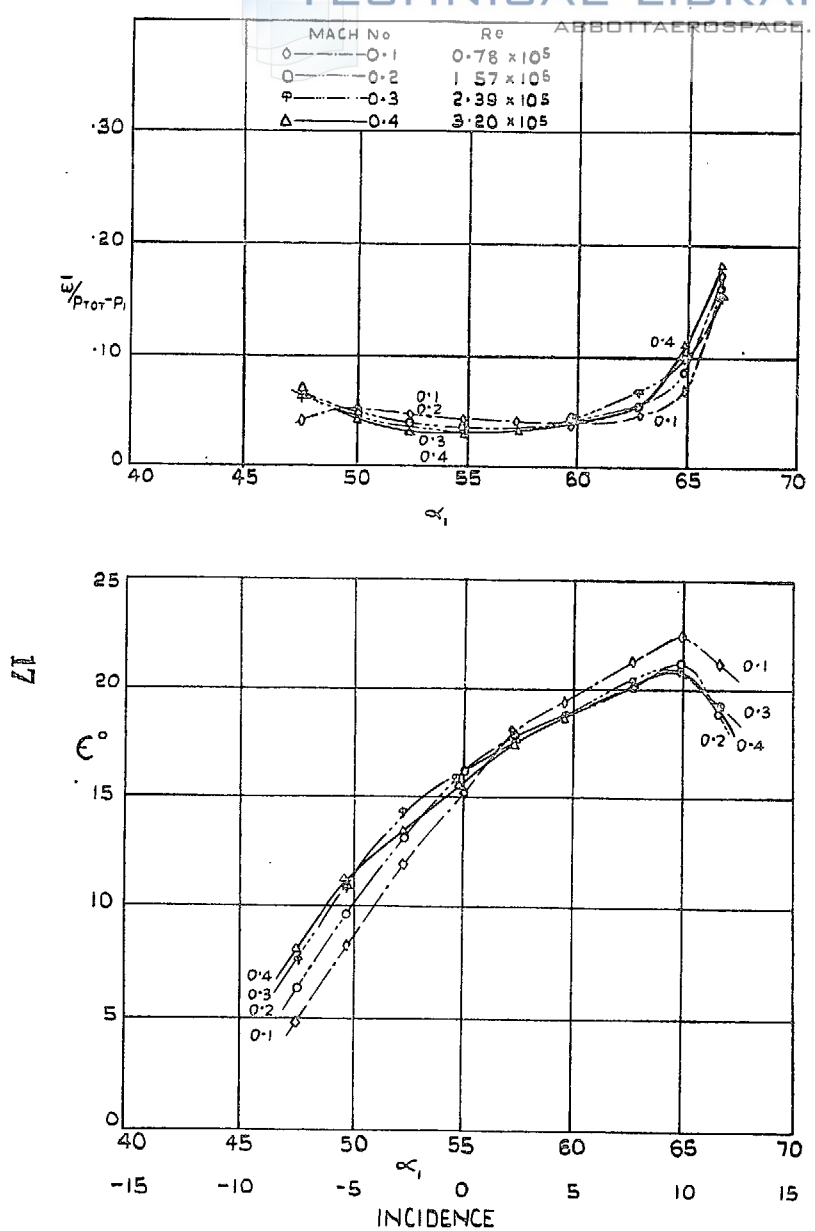

FIG. 11. Cascade 8·5CT(S)/25C50.
$\frac{\bar{\omega}}{P_{tot} - P_1}$ and ε against α_1. Low Mach numbers.

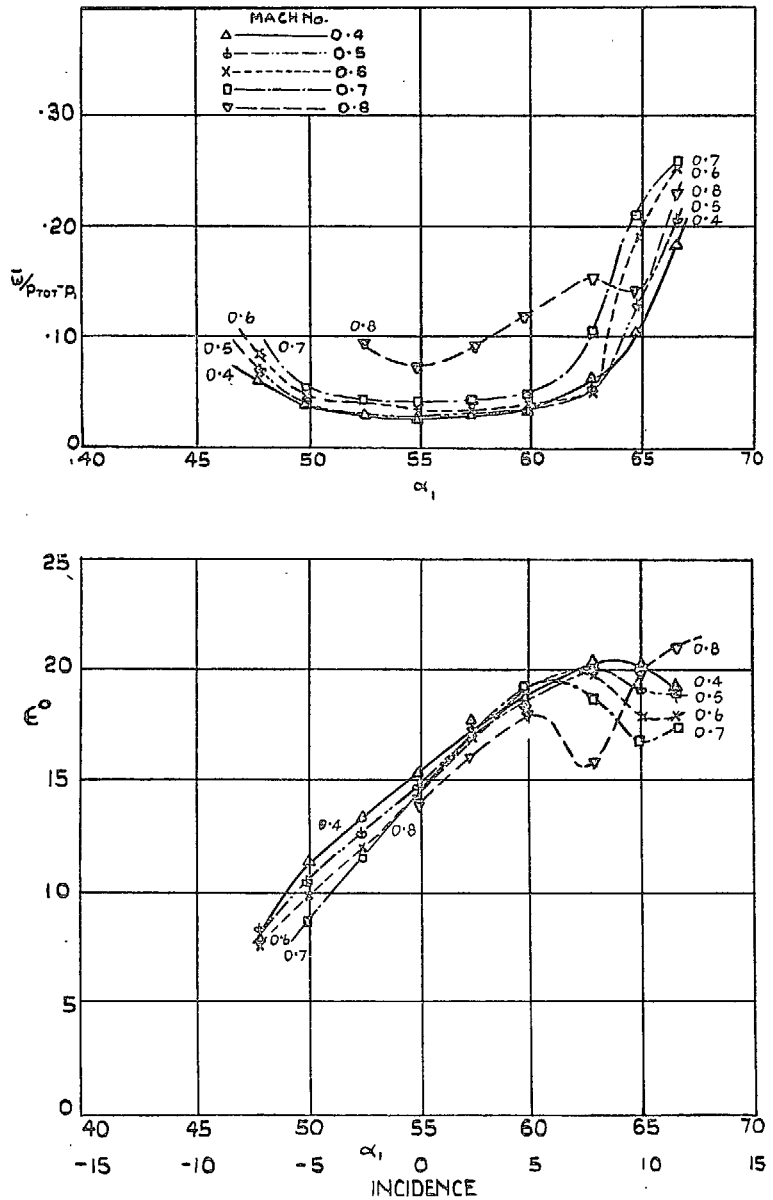

FIG. 12. Cascade 8·5CT(S)/25C50.
$\frac{\bar{\omega}}{P_{tot} - P_1}$ and ε against α_1. High Mach numbers.

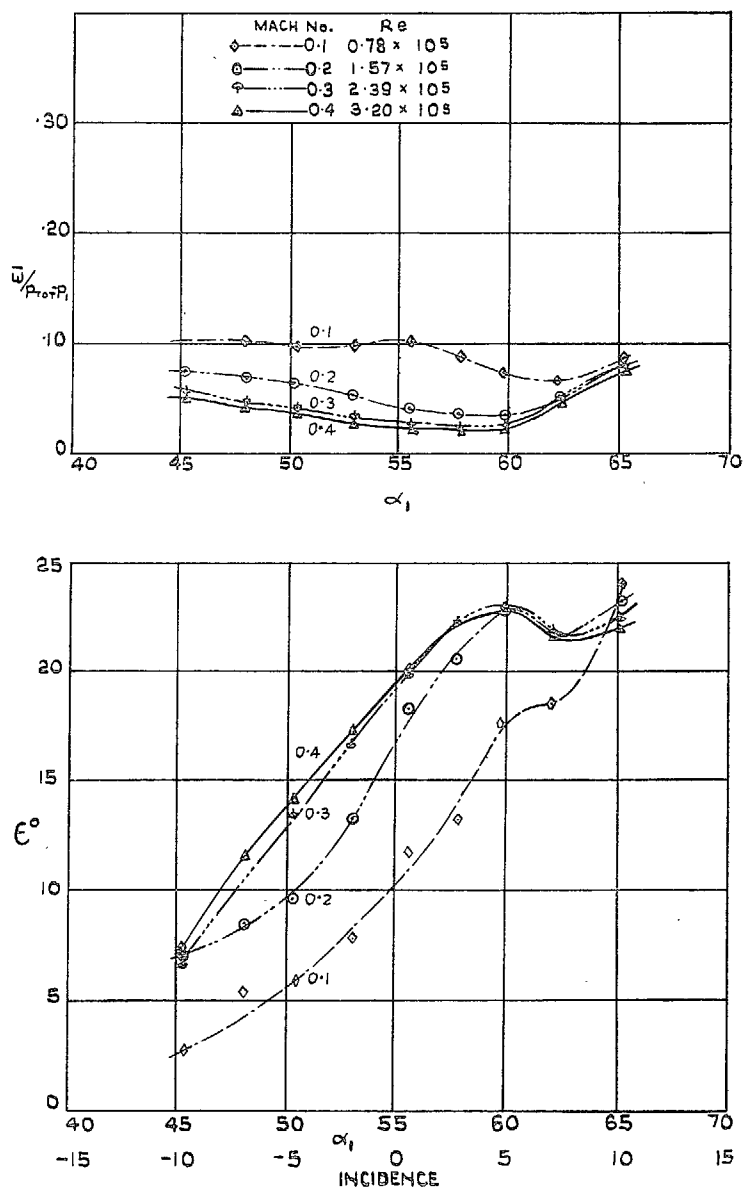

FIG. 13. Cascade 10·5/2A/25C50.
$\frac{\bar{\omega}}{P_{tot} - P_1}$ and ε against α_1. Low Mach numbers.

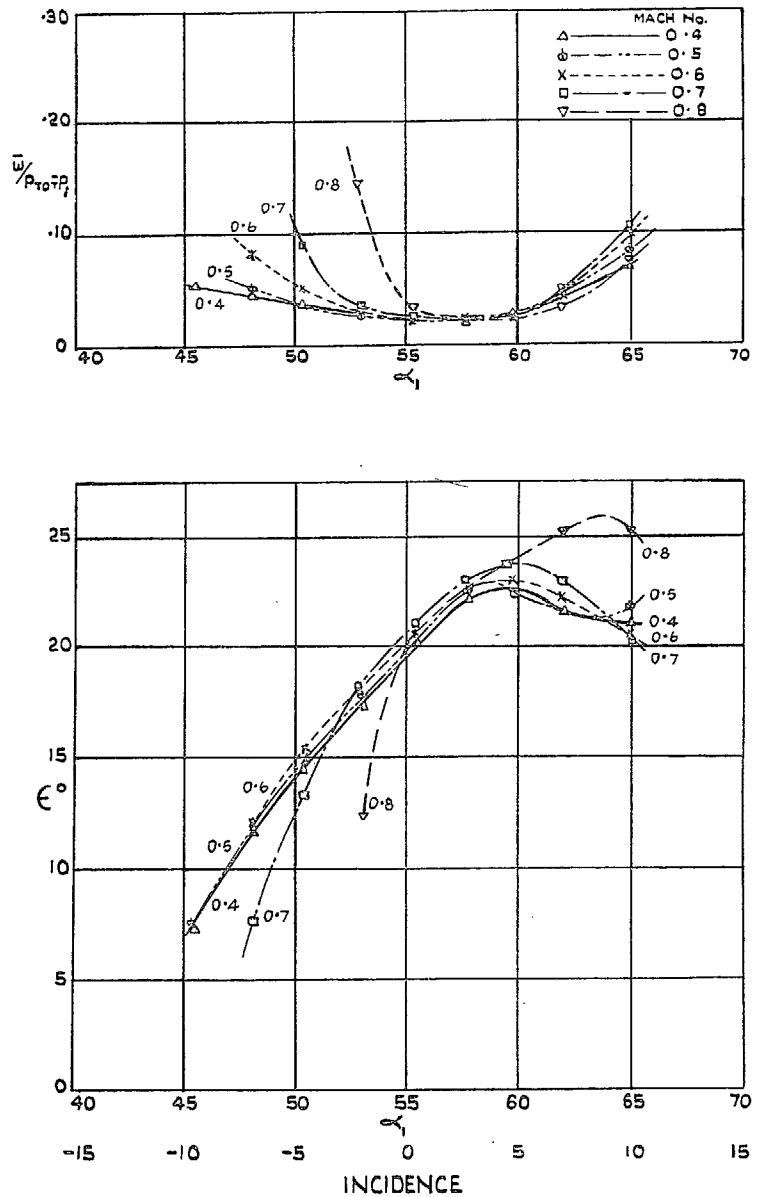

FIG. 14. Cascade 10·5/2A/25C50.
$\frac{\bar{\omega}}{P_{tot} - P_1}$ and ε against α_1. High Mach numbers.

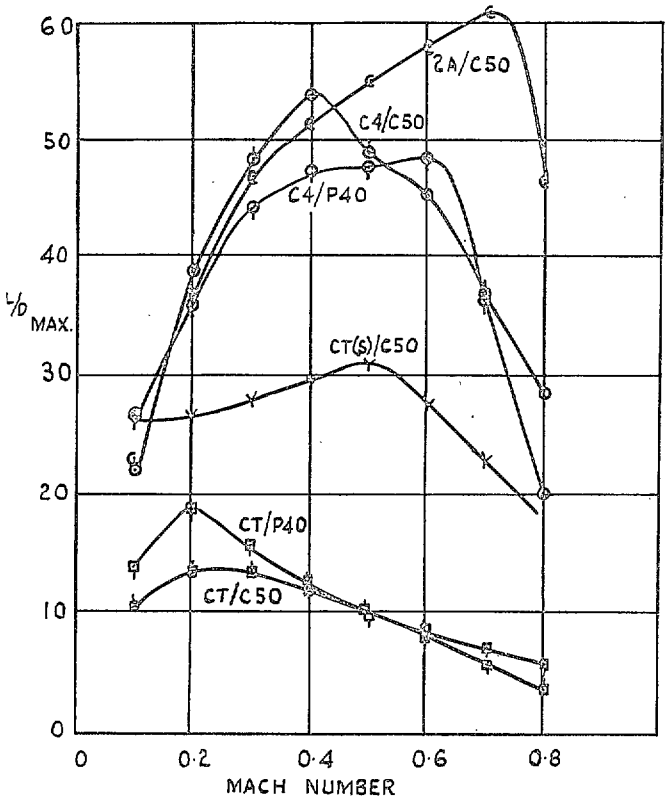

L/D_{max} against Mach number.

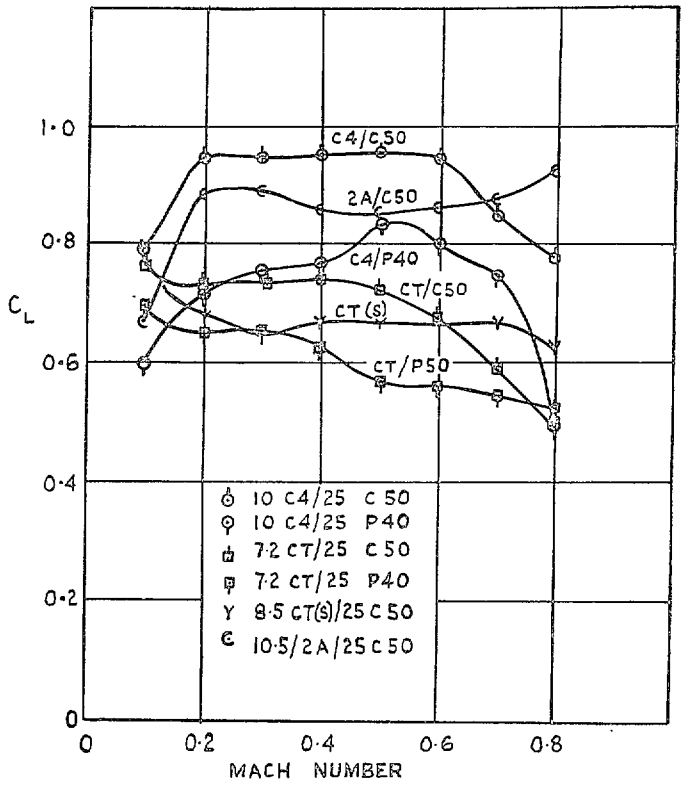

C_L at L/D_{max} against Mach number.

FIG. 15.

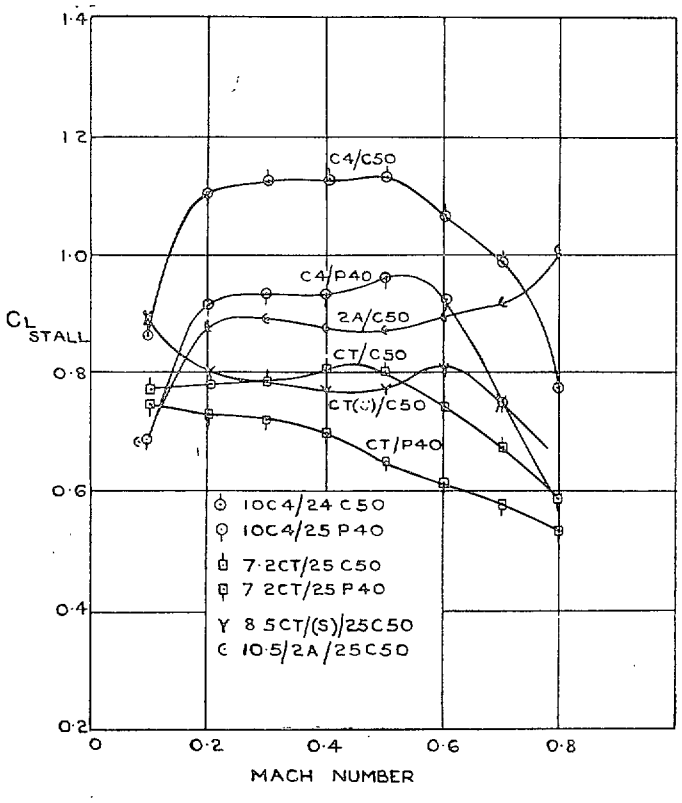

Stalling C_L against Mach number.

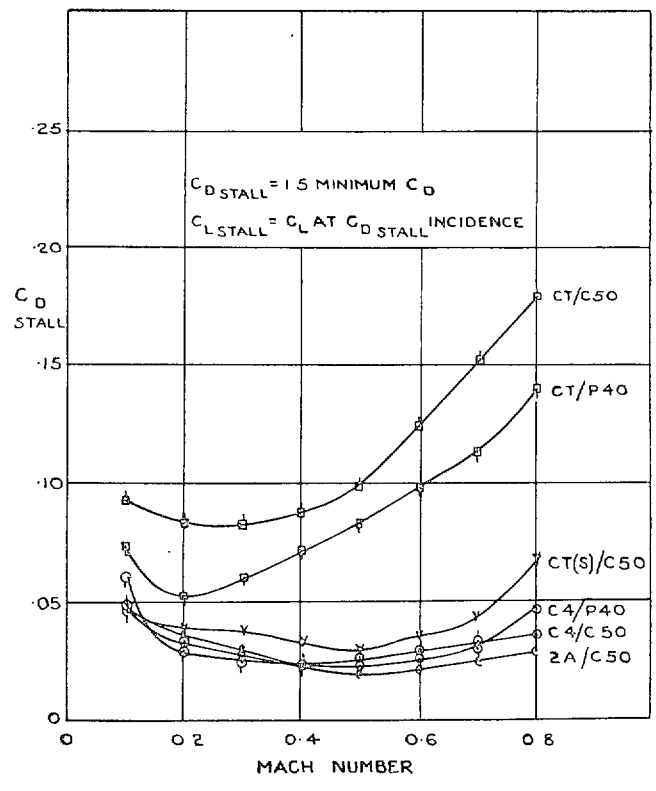

Stalling C_D against Mach number.

FIG. 16.

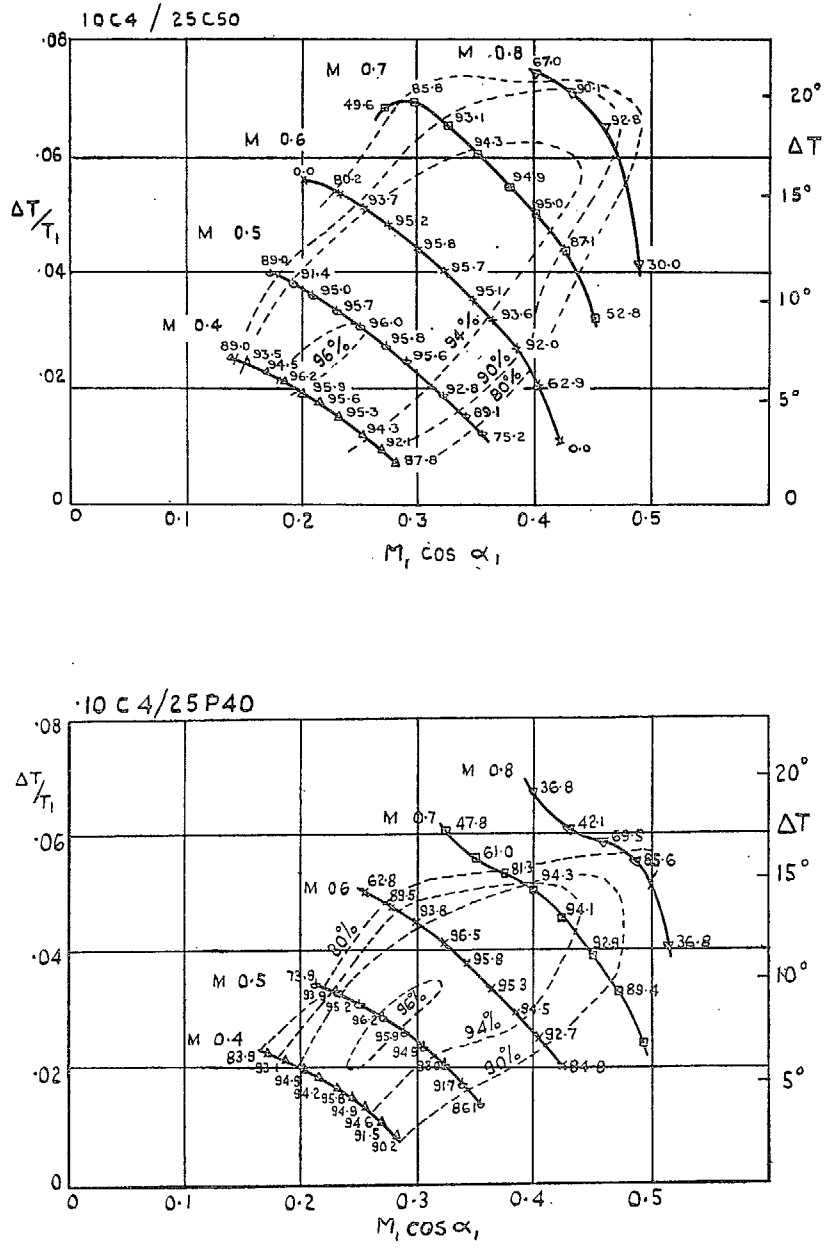

FIG. 17. $\Delta T/T_1$ against $M \cos \alpha_1$.
Values are for one blade row, *i.e.*, half a stage.
———— Constant inlet Mach number.
– – – – – Constant two-dimensional efficiency.
ΔT scale for $T_1 = 288°$ K.

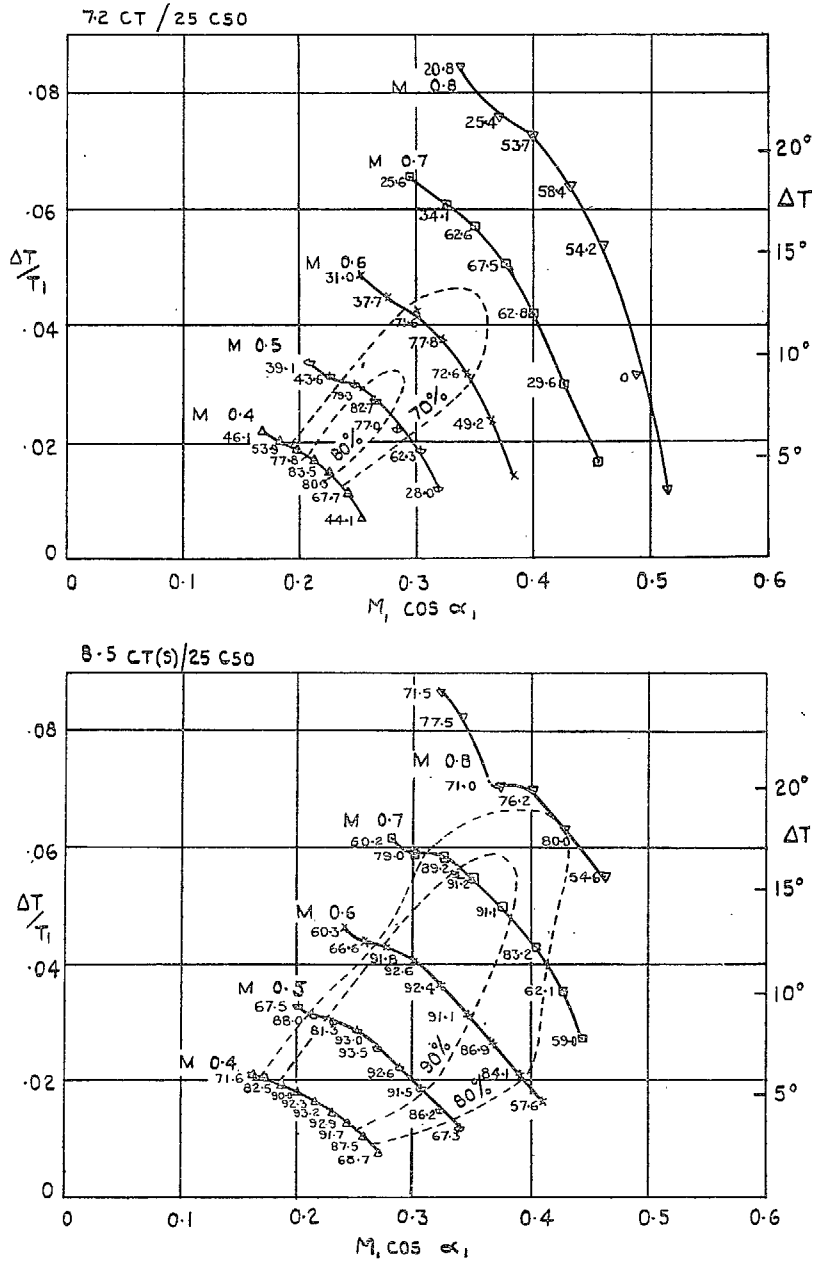

FIG. 18. $\Delta T/T_1$ and $\Delta P/P_1$ against $M \cos \alpha_1$.
Values are for one blade row, *i.e.*, half a stage.
———— Constant inlet Mach number.
– – – – – Constant two-dimensional efficiency
ΔT scale for $T_1 = 288°$ K.

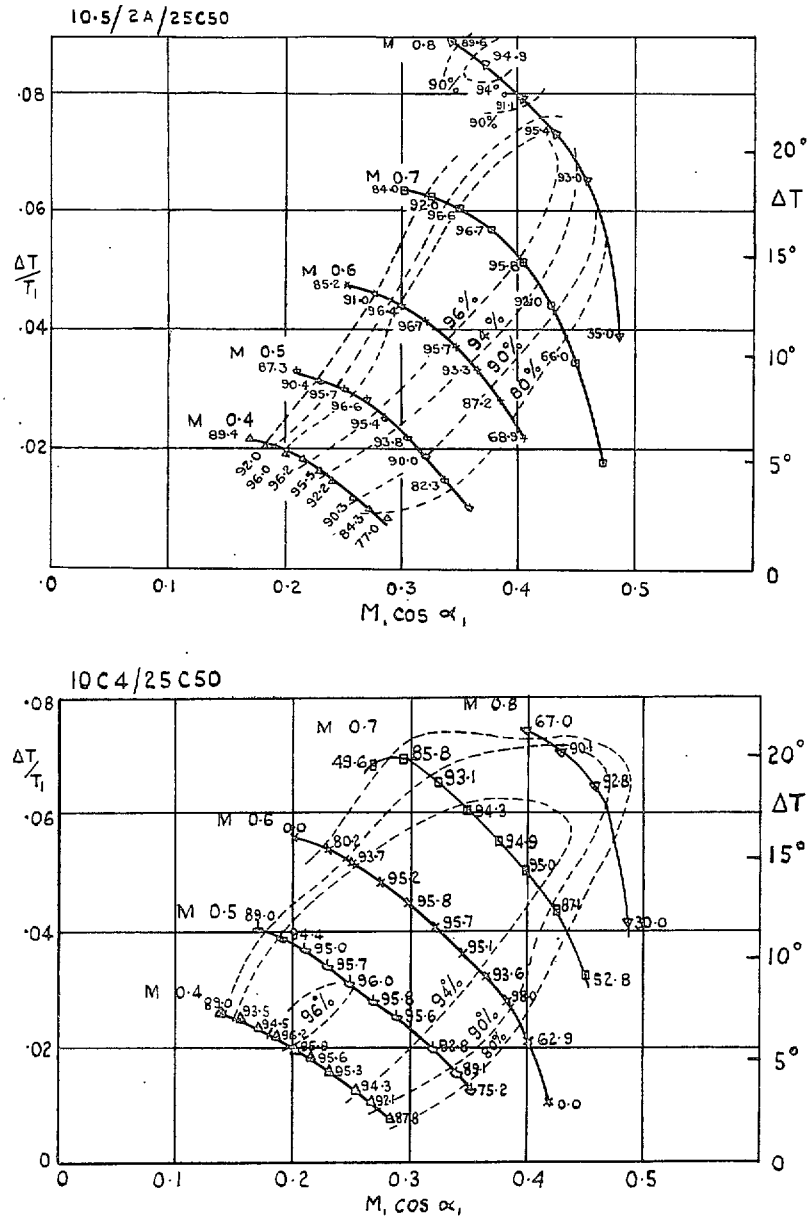

FIG. 19. $\Delta T/T_1$ against $M \cos \alpha_1$.
Values are for one blade row, *i.e.*, half a stage.
———— Constant inlet Mach number.
– – – – – Constant two-dimensional efficiency.
ΔT scale for $T_1 = 288°$ K.

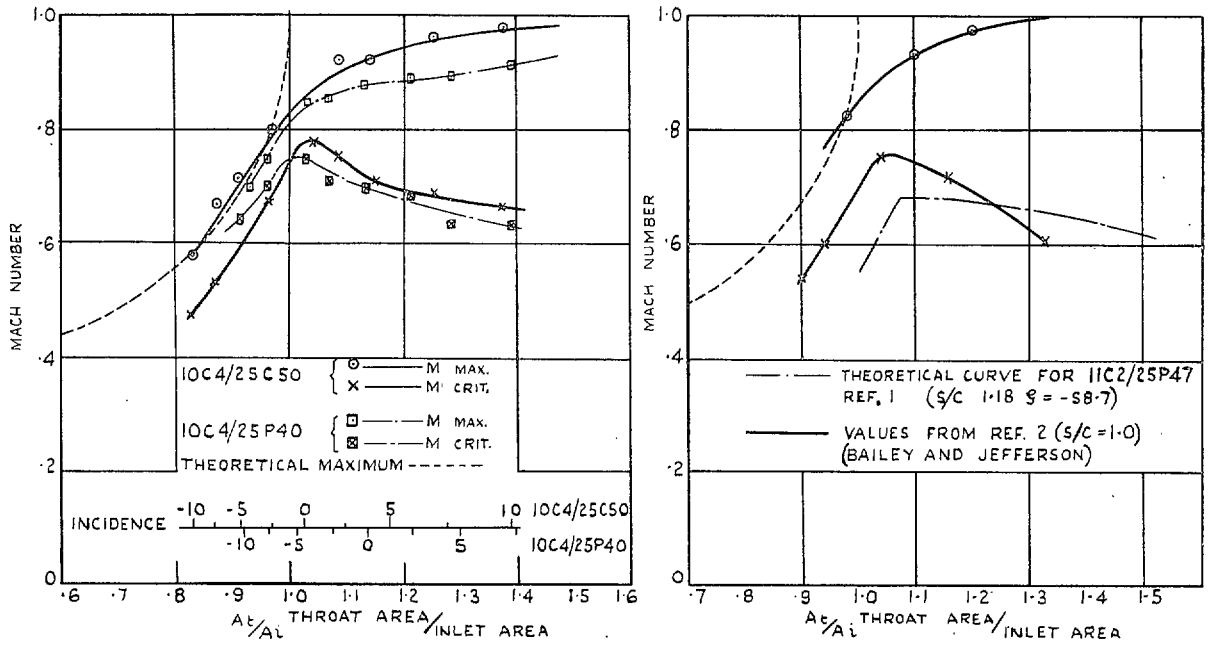

FIG. 20. Maximum and critical Mach numbers.
Maximum M based on zero pressure rise (measured). Critical M based on $1 \cdot 5 \times$ minimum loss.

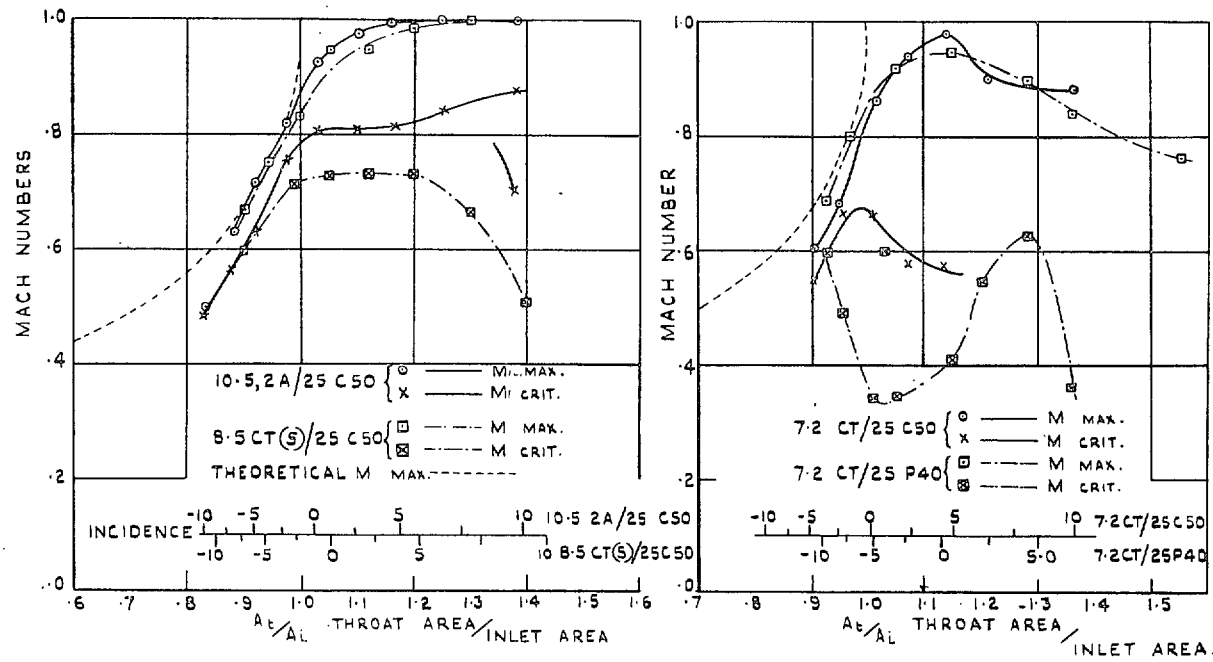

FIG. 21. Maximum and critical Mach numbers.
Maximum M based on zero pressure rise (measured). Critical M based on $1 \cdot 5 \times$ minimum loss.

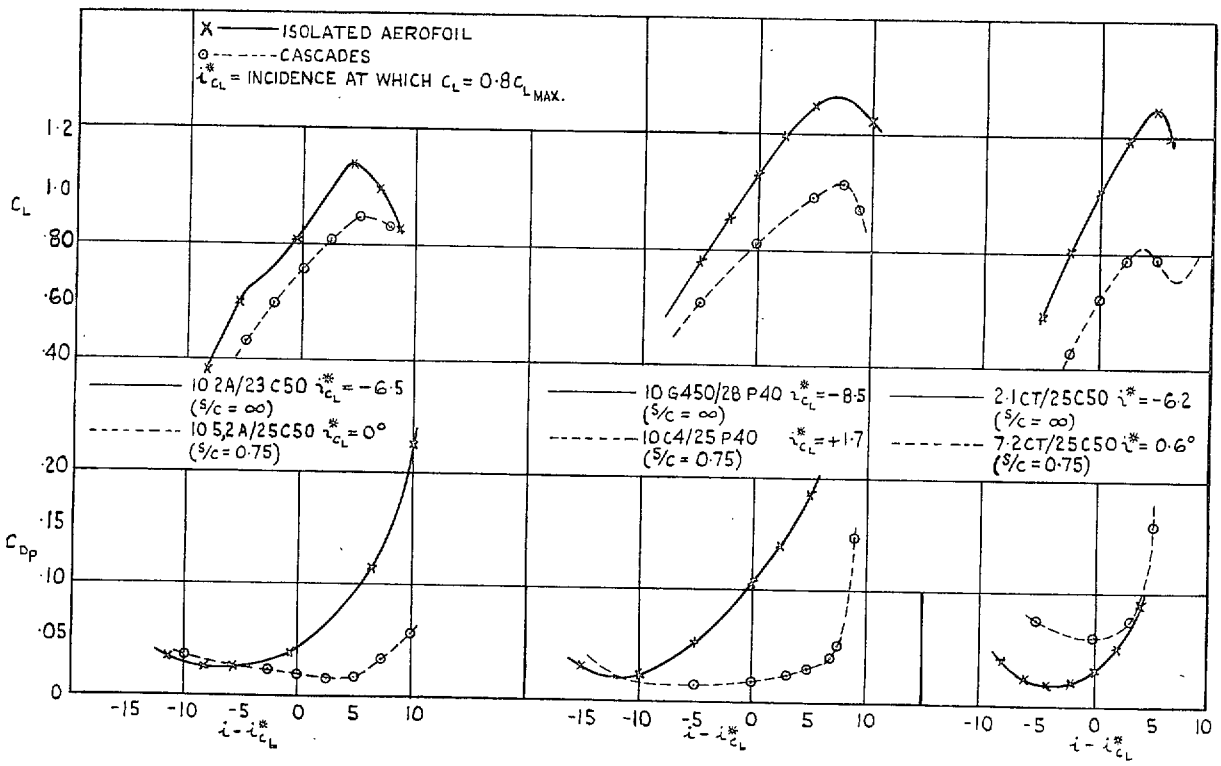

FIG. 22. Performance of blades, isolated and in cascade.

(52569) Wt. 15/680 K.9 3/55 Hw.

PRINTED IN GREAT BRITAIN

Publications of the Aeronautical Research Council

ANNUAL TECHNICAL REPORTS OF THE AERONAUTICAL RESEARCH COUNCIL (BOUND VOLUMES)

1936 Vol. I. Aerodynamics General, Performance, Airscrews, Flutter and Spinning. 40*s*. (41*s*. 1*d*.)
Vol. II. Stability and Control, Structures, Seaplanes, Engines, etc. 50*s*. (51*s*. 1*d*.)

1937 Vol. I. Aerodynamics General, Performance, Airscrews, Flutter and Spinning. 40*s*. (41*s*. 1*d*.)
Vol. II. Stability and Control, Structures, Seaplanes, Engines, etc. 60*s*. (61*s*. 1*d*.)

1938 Vol. I. Aerodynamics General, Performance, Airscrews. 50*s*. (51*s*. 1*d*.)
Vol. II. Stability and Control, Flutter, Structures, Seaplanes, Wind Tunnels, Materials. 30*s*. (31*s*. 1*d*.)

1939 Vol. I. Aerodynamics General, Performance, Airscrews, Engines. 50*s*. (51*s*. 1*d*.)
Vol. II. Stability and Control, Flutter and Vibration, Instruments, Structures, Seaplanes, etc. 63*s*. (64*s*. 2*d*.)

1940 Aero and Hydrodynamics, Aerofoils, Airscrews, Engines, Flutter, Icing, Stability and Control. Structures, and a miscellaneous section. 50*s*. (51*s*. 1*d*.)

1941 Aero and Hydrodynamics, Aerofoils, Airscrews, Engines, Flutter, Stability and Control. Structures. 63*s*. (64*s*. 2*d*.)

1942 Vol. I. Aero and Hydrodynamics, Aerofoils, Airscrews, Engines. 75*s*. (76*s*. 3*d*.)
Vol. II. Noise, Parachutes, Stability and Control, Structures, Vibration, Wind Tunnels 47*s* 6*d*. (48*s*. 7*d*.)

1943 Vol. I. Aerodynamics, Aerofoils, Airscrews. 80*s*. (81*s*. 4*d*.)
Vol. II. Engines, Flutter, Materials, Parachutes, Performance, Stability and Control, Structures 90*s*. (91*s*. 6*d*.)

1944 Vol. I. Aero and Hydrodynamics, Aerofoils, Aircraft, Airscrews, Controls. 84*s*. (85*s*. 8*d*.)
Vol. II. Flutter and Vibration, Materials, Miscellaneous, Navigation, Parachutes, Performance, Plates and Panels, Stability, Structures, Test Equipment, Wind Tunnels. 84*s*. (85*s*. 8*d*.)

Annual Reports of the Aeronautical Research Council—

1933–34	1*s*. 6*d*. (1*s*. 8*d*.)	1937	2*s*. (2*s*. 2*d*.)
1934–35	1*s*. 6*d*. (1*s*. 8*d*.)	1938	1*s*. 6*d*. (1*s*. 8*d*.)
April 1, 1935 to Dec. 31, 1936	4*s*. (4*s*. 4*d*.)	1939–48	3*s*. (3*s*. 2*d*.)

Index to all Reports and Memoranda published in the Annual Technical Reports, and separately—

April, 1950 - - R. & M. No. 2600. 2*s*. 6*d*. (2*s*. 7½*d*.)

Author Index to all Reports and Memoranda of the Aeronautical Research Council—

1909–1949. R. & M. No. 2570. 15*s*. (15*s*. 3*d*.)

Indexes to the Technical Reports of the Aeronautical Research Council—

December 1, 1936 — June 30, 1939.	R. & M. No. 1850.	1*s*. 3*d*. (1*s*. 4½*d*.)
July 1, 1939 — June 30, 1945.	R. & M. No. 1950.	1*s*. (1*s*. 1½*d*.)
July 1, 1945 — June 30, 1946.	R. & M. No. 2050.	1*s*. (1*s*. 1½*d*.)
July 1, 1946 — December 31, 1946.	R. & M. No. 2150.	1*s*. 3*d*. (1*s*. 4½*d*.)
January 1, 1947 — June 30, 1947.	R. & M. No. 2250.	1*s*. 3*d*. (1*s*. 4½*d*.)
July, 1951.	R. & M. No. 2350.	1*s*. 9*d*. (1*s*. 10½*d*.)

Prices in brackets include postage.

Obtainable from

HER MAJESTY'S STATIONERY OFFICE

York House, Kingsway, London, W.C.2: 423 Oxford Street, London, W.1 (Post Orders: P.O. Box 569, London, S.E.1); 13a Castle Street, Edinburgh 2; 39 King Street, Manchester 2; 2 Edmund Street, Birmingham 3; 109 St. Mary Street, Cardiff: Tower Lane, Bristol, 1; 80 Chichester Street, Belfast, or through any bookseller

S.O. Code No. 23-2743